MEASUREMENT AND QCD-ANALYSIS OF THE PROTON STRUCTURE FUNCTION $F_2(x, Q^2)$ AT HERA

FRANK LEHNER
on behalf of the H1 and ZEUS Collaboration
DESY
NOTKESTR. 85
D-22607 HAMBURG
GERMANY
E-mail: lehnerf@mail.desy.de

New results on measurements of the proton structure function $F_2(x,Q^2)$ from H1 and ZEUS at HERA are presented. The data were collected in 1995 and 1996 covering the range $0.16 \leq Q^2 \leq 90$ GeV^2 and reaching values of x down to $2 \cdot 10^{-6}$. Contrary to observations at values of $Q^2 \sim 10$ GeV^2, the rise in F_2 with decreasing x is found to be weaker at low Q^2. Conventional NLO QCD evolution equations provide a good description of the data down to Q^2 of 1.5 GeV^2. From scaling violations a gluon density is derived, which rises strongly towards small x. In addition, cross section measurements from H1 at high y allow a determination of F_L in the HERA range.

1 Introduction

The two experiments H1 and ZEUS at the electron-proton collider HERA have been collecting data since 1992. The increased center-of-mass energy $\sqrt{s} \approx 300$ GeV extends the accessible kinematic region in x and Q^2 by two orders of magnitude over previous fixed target experiments. First results of the proton structure function from HERA demonstrated [1] that F_2 rises steeply with decreasing x. The rise has been verified with much greater precision with data from 1994 [2,3] based on a collected luminosity of 3 pb^{-1}. These data cover the range $1.5 \leq Q^2 \leq 5000$ GeV^2 and $3 \cdot 10^{-5} \leq x \leq 0.35$. It was found, that the data can be successfully described by perturbative QCD in the measured range, using the NLO DGLAP evolution equations.

In this paper, proton structure function measurements covering the range $0.16 \leq Q^2 \leq 90$ GeV^2 are presented. The access to very low $Q^2 \leq 1$ GeV^2 was possible by positioning new measuring devices in the backward (electron beam direction) region of the detector. The measured behavior of the structure function at $Q^2 \leq 1$ GeV^2 can be compared with phenomenological models based on Regge expectations [4]. In addition, these data can experimentally establish and probe the transition between the region of perturbative QCD and Regge phenomenology. New preliminary results on F_2 in the Q^2 range $2 \leq Q^2 \leq 90$ GeV^2 from data taken in 1995 and 1996 with the H1 detector are presented. While validating the previous H1 measurements, these data also represent an important improvement in the reached statistical and systematic precision. The extraction of the gluon density from NLO QCD fits to F_2 data and a new determination of the longitudinal structure function F_L are presented.

2 Deep Inelastic Scattering

The double differential cross section for neutral current deep inelastic lepton($e^{\pm}$)-proton scattering, where only a single chargeless boson (γ, Z^0) is exchanged, can be expressed in terms of the proton structure functions F_2, F_L and xF_3 as

$$\frac{d^2\sigma^{e^{\pm}p}}{dxdQ^2} = \frac{2\pi\alpha^2}{Q^4 x}(Y_+ F_2(x,Q^2) - y^2 F_L(x,Q^2) \mp Y_- xF_3(x,Q^2)), \qquad (1)$$

where $Y_{\pm} = 1 \pm (1-y)^2$. The squared four-momentum transfer is given by Q^2 and x represents the Bjorken scaling variable. The center of mass energy squared is $s = 4E_pE_e$, where E_e and E_p are the electron and proton beam energies respectively. The inelasticity y can be determined from $Q^2 = sxy$ and represents the fractional energy transfer in the rest system of the proton.

In the Quark-Parton-Model (QPM) F_2 can be expressed in terms of the parton densities $q_i, \overline{q_i}$ in the proton as $F_2 = \sum_{i=q}^{n_f} e_i^2(q(x)+\overline{q}(x))$ assuming single photon exchange only. The longitudinal structure function F_L is directly connected to the cross section $\sigma_L^{\gamma^* p}$ of longitudinal polarized photons on protons. The value of F_L is generally small and, since its contribution to the cross section is diminished by the factor y^2 in Eq. (1), is only important for high $y \geq 0.6$. In order to determine F_2 from a measurement of the differential cross section, QCD calculations for F_L at $Q^2 > 1$ GeV^2 and phenomenological models at lower Q^2 are used. For increasing Q^2 the weak part of the neutral current must be included in the definition of the structure functions, i.e. additional terms due to $\gamma - Z^0$ interference and Z^0-exchange. The structure function xF_3 contains such terms only and can be neglected for $Q^2 \leq 5000$ GeV^2. Note that xF_3 and F_L have not yet been measured directly at HERA.

Finally one defines the total virtual photon-proton ($\gamma^* p$) cross section for longitudinal and transverse polarized photons as

$$\sigma_{tot}^{\gamma^* p} = \sigma_T^{\gamma^* p} + \sigma_L^{\gamma^* p} \simeq \frac{4\pi^2\alpha}{Q^2}F_2. \qquad (2)$$

3 New HERA results of F_2

The HERA experiments H1 and ZEUS allow an extension of the kinematic coverage towards very large values in the momentum transfer Q^2 and very low values in the Bjorken scaling variable x compared to previous fixed target experiments. The HERA data span now 6 orders of magnitude in x and 5 orders of magnitude in Q^2. In the year 1995, both H1 and ZEUS improved their detectors to allow measurements of electron scattering angles close to zero. ZEUS added a special detector (BPC) near the beam pipe in the electron beam (backward) direction allowing F_2 measurements [5] at lower Q^2 down to $Q^2 = 0.11$ GeV^2. The H1 collaboration replaced the previous electromagnetic calorimeter in the backward direction by a lead/scintillating fiber calorimeter (SPACAL) [6] and measured F_2 down to $Q^2 = 0.35$ GeV^2 [7] using data collected during a short period in 1995 when the ep collision vertex was shifted by 70 cm in the proton direction. The results of these measurements are discussed in Sec. 6. In 1996 H1 performed cross section measurements [8] up to $y = 0.82$, a region where the sensitivity to the longitudinal proton structure function F_L is enlarged.

In Fig. 1 new preliminary H1 measurements from data taken in the 1995 and 1996 are shown. The data points cover the Q^2 range $2 \leq Q^2 \leq 90$ GeV^2. With an accuracy of about 8-12% at low Q^2 ($Q^2 \leq 8.5$ GeV^2), these are the most precise data obtained by H1 in this kinematic region so far. The full line in Fig. 1 depicts the result of a QCD fit to the H1 data with the goal to determine the gluon density. The details of the QCD analysis are described in the next section.

4 Determination of the gluon density

In perturbative QCD the Q^2 evolutions of parton densities are governed by the DGLAP equations [9]

$$\frac{\partial}{\partial t} q_{NS}(x,t) = \frac{\alpha_s(t)}{2\pi} P_{qq}^{NS} \otimes q_{NS}(y,t) \quad \text{with} \quad t = \log \frac{Q^2}{\Lambda_{QCD}^2}, \tag{3}$$

$$\frac{\partial}{\partial t} \begin{pmatrix} \Sigma(x,t) \\ g(x,t) \end{pmatrix} = \frac{\alpha_s(t)}{2\pi} \begin{pmatrix} P_{qq} & P_{qg} \\ P_{gq} & P_{gg} \end{pmatrix} \otimes \begin{pmatrix} \Sigma(y,t) \\ g(y,t) \end{pmatrix}, \tag{4}$$

where $\otimes$ stands for a convolution integral and α_s is the strong coupling constant. The non-singlet density xq_{NS} is given by $xq_{NS} = \sum_{i=1}^{n_f}(xq_i - x\overline{q_i}) = xu_{val} + xd_{val}$, where u_{val} and d_{val} denote the valence quarks in the proton. Non-singlet partons evolve independently in the DGLAP equation. The second equation couples the singlet density Σ to the gluon density xg. The splitting

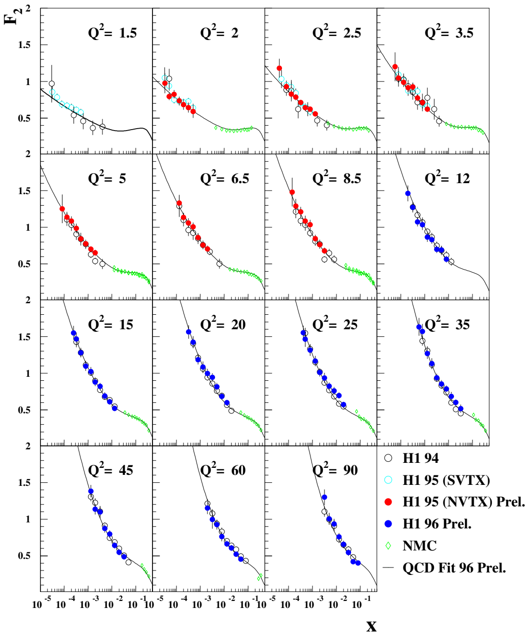

Figure 1: New preliminary H1 measurements on F_2 using data from 1995 and 1996. The full line corresponds to a QCD fit to the data (see Sec. 4)

functions P_{ij} are obtained by a perturbative expansion in a specific factorization and renormalization scheme and are presently known to next-to-leading order (NLO). The factorization theorem defines the structure function F_2 as a convolution of the parton densities and coefficient functions C_i:

$$\frac{1}{x}F_2(x,Q^2) = \sum_{i=1}^{n_f} e_i^2 C_q(x,Q^2) \otimes (q_i(x,Q^2) + \overline{q_i}(x,Q^2)) + C_g(x,Q^2) \otimes g(x,Q^2). \tag{5}$$

The essence of a QCD analysis of structure functions is the comparison of their Q^2 dependence with the prediction of perturbative QCD. The DGLAP evolution equations are solved by assuming input parton distributions at some starting scale Q_0^2. The input parameters are then adjusted such that the computed structure function fits the data at all x and Q^2. In such a procedure the value of Q_0^2 is arbitrary; in practice one often chooses a value typical for the data.

Both the H1 and ZEUS collaborations performed NLO QCD fits to their F_2 data with the goal to determine the gluon distribution at low x. The ZEUS fit [10] used the ZEUS F_2^p data [2] in the range $1.5 \leq Q^2 \leq 5000$ GeV^2 and NMC data[12] on F_2^p and F_2^d to constrain the fit at higher x. To remove possible higher twist effects at large x, the NMC data below $Q^2 = 4$ GeV^2 were discarded. The input scale Q_0^2 was chosen to be 7 GeV^2, at which the gluon distribution xg, the singlet distribution $x\Sigma$, and the difference of up and down quarks in the proton $x\Delta_{ud}$ were parameterized as

$$
\begin{aligned}
xg(x, Q_0^2) &= A_g x^{\delta_g}(1-x)^{\eta_g}(1+\gamma_g x), & (6)\\
x\Sigma(x, Q_0^2) &= A_S x^{\delta_S}(1-x)^{\eta_S}(1+\gamma_S x+\epsilon_S\sqrt{x}), & (7)\\
x\Delta_{ud}(x, Q_0^2) &= A_{ns} x^{\delta_{ns}}(1-x)^{\eta_{ns}}. & (8)\\
& & (9)
\end{aligned}
$$

In the ZEUS fit the strange quark distribution s is assumed to be 20% of the total sea at $Q^2 = 4$ GeV^2. The sea is obtained by subtracting the MRSD0' valence distribution [11] from the parameterized singlet distribution. The value of the strong coupling constant α_s at the M_Z scale was chosen to be 0.113.

In the present update of the published H1 fit results [2] the input scale of the DGLAP evolution was set to $Q_0^2 = 1$ GeV^2. The fit included all H1 data[3,8] with $1.5 \leq Q^2 \leq 5000$ GeV^2, except those with $y > 0.6$. Additionally, data from NMC [13] and BCDMS [14] on both proton and deuteron targets have been included. A cut on the fixed target experiments, NMC and BCDMS, of $x \geq 0.5$ and $Q^2 \geq 5$ GeV^2 was employed to remove possible higher twist corrections and keep target mass corrections [15] as low as possible. The input parton distributions at $Q_0^2 = 1$ GeV^2 were parameterized in the following way:

$$
\begin{aligned}
xg(x, Q_0^2) &= A_g x^{B_g}(1-x)^{C_g}, & (10)\\
xu_v(x, Q_0^2) &= A_u x^{B_u}(1-x)^{C_u}(1+D_u x+E_u\sqrt{x}), & (11)\\
xd_v(x, Q_0^2) &= A_d x^{B_d}(1-x)^{C_d}(1+D_d x+E_d\sqrt{x}), & (12)\\
xS(x, Q_0^2) &= A_S x^{B_S}(1-x)^{C_S}(1+D_S x+E_S\sqrt{x}). & (13)
\end{aligned}
$$

where $S = \overline{u} + \overline{d}$ defines the non strange sea distribution. For simplicity $\overline{u} = \overline{d}$ is assumed and the strange quark distribution s is taken to be $2s = \overline{u}$. The value of α_s at the M_Z scale was set to 0.118.

Both DGLAP evolutions use the $\overline{MS}$ renormalization scheme for three light flavors (u, d, s), adding the charm contribution from a NLO calculation of the boson gluon fusion (BGF) process [16] with m_c set to 1.5 GeV. The momentum sum rule is applied in both fits to constrain the parameters of the gluon normalization A_g. Further, H1 employs the two valence counting rules to fix the normalization parameters A_u and A_d. In both fits the normalization of all included data sets were allowed to vary by the amount of the quoted normalization uncertainties.

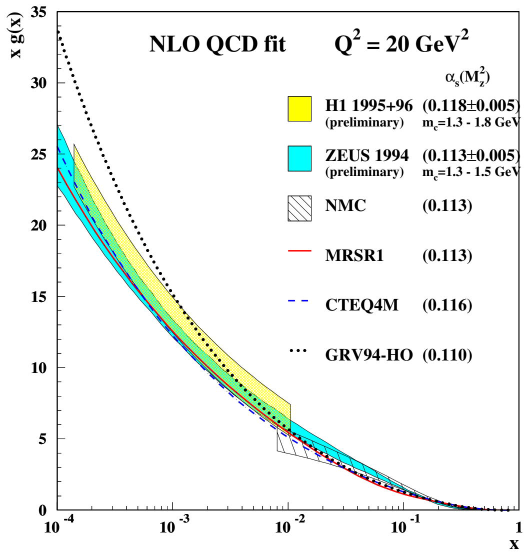

Figure 2: Gluon distributions at $Q^2 = 20$ GeV^2 from the HERA NLO QCD fits to structure function data. The error bands include the statistical and systematic errors and also the uncertainties due to an α_s variation and due to the charm quark mass m_c uncertainty. The gluon distribution from a QCD fit [17] to NMC data is also shown at higher x. The MRSR1, CTEQ4M and GRV94-HO parameterizations are shown for comparison.

The resulting gluon distributions [8,10] extracted from the NLO fits to H1 and ZEUS data are shown in Fig. 2. The error bands account for statistical and systematic errors including correlations, variations in $\alpha_s(M_Z)$ by ± 0.005 and variations in the charm quark mass ($m_c = 1.5 \pm 0.3$ for the H1 fit; $1.3 < m_c < 1.5$ GeV for the ZEUS fit). The agreement between the fit results is very good. At the lowest x values ($x \sim 10^{-4}$) the gluon density is now accurate with a precision of about 15%. The steeply rising gluon distribution towards low x, as found by H1 and ZEUS, is in good agreement with the results of global QCD analyses carried out by MRS [18] and CTEQ [19] whereas the gluon density obtained from the dynamical evolution by GRV [20] is too steep.

5 Extraction of F_L

The H1 measurements [3,7,8] of F_2, shown in figure 1 and discussed in Sec. 3, were limited to y values below 0.7. At large y, however, the effect of the F_L contribution to the double differential cross section as seen in Eq. (1) becomes important. The H1 Collaboration has used, for their 1994 data, a new method [21] to extract F_L in the high y region ($y \sim 0.7$; $8.5 \leq Q^2 \leq 35$ GeV^2; $1.3 \cdot 10^{-4} \leq x \leq 5.5 \cdot 10^{-4}$). In order to determine the F_2 contribution to the cross section at high y, F_2 data at $y < 0.35$, where F_2 is safely measured, is fit using a NLO QCD procedure described in Sec. 4. The fit is then extrapolated, by standard DGLAP evolution, to the region of high y to obtain the F_2 contribution to the total cross section. F_L is extracted by taking the difference between the measured cross section and the extrapolated F_2. Although this method assumes that F_2 obeys DGLAP QCD evolution, it makes no assumption about F_L.

With data recorded in 1996, in the range $0.65 \leq y \leq 0.85$ and $12 \leq Q^2 \leq 35$ GeV^2, H1 repeated the extraction of F_L [8] from their measured cross sections. The F_2 extrapolation was based on a QCD fit to the new preliminary H1 data (1995, 1996) at $y < 0.35$ only and to the NMC and BCDMS measurements. The extracted F_L values from the 1996 data are shown for two y bins in Fig. 3

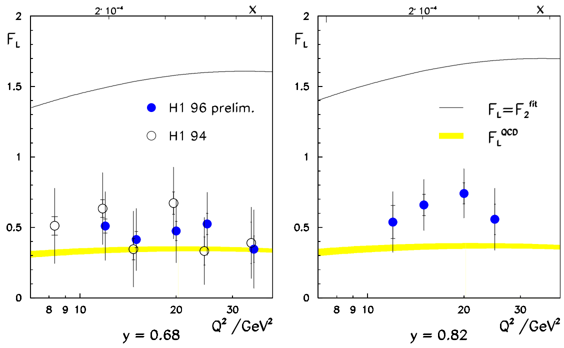

Figure 3: Longitudinal structure function $F_L = \frac{Y_+}{y^2}(F_2^{fit} - \sigma/\kappa)$, where $\kappa = (2\pi\alpha^2 Y_+)/(Q^4 x)$ and $Y_+ = 1 + (1-y)^2$, determined as function of Q^2 or $x = Q^2/sy$ for $y = 0.68$ and $y = 0.82$. The closed points represent the preliminary H1 (1996) result while the open points are the published H1 (1994) data.

as closed points compared to the previous published F_L result [21] represented as open points. For $y = 0.68$ the new result is in good agreement with the 1994 data. The total error of F_L includes three different sources: the uncorrelated part of the systematic error of the high y cross section measurement, these systematic error components of the cross section that are correlated to the error on the input data to the QCD fit, and the errors due to different assumptions inherent in the QCD fit. From these three error contributions, the genuine high y cross section uncertainty is the dominating one.

The calculation of F_L based on the QCD fit is shown in Fig. 3 by a shaded band. The uncertainty of this calculation, based on the experimental errors of the input data and on variations of α_s and m_c similar to the NLO QCD fit presented in sec. 4, is on the order of 6%. The data points are in agreement with the QCD expectation, however, they tend to be systematically higher than the calculation (note that points at given y are highly correlated). This tendency is more pronounced in the highest y bin of $y = 0.82$, which was obtained with the 1996 data.

A direct measurement of F_L at HERA which is free of any input assumptions is foreseen by measuring the ep inclusive cross section at different incident proton beam energies. An independent and accurate determination of F_L would yield particularly interesting results for new QCD studies.

6 The very low Q^2 region

Two basic methods were used to extend the measurements of F_2 to lower values of Q^2 [5,7]. To increase the acceptance of electrons with smaller scattering angles, a part of the HERA 1995 run was performed with the interaction region shifted by about 70 cm in the forward direction. Additionally in 1994/1995, ZEUS installed a small tungsten-scintillator calorimeter (BPC) behind the rear Calorimeter adjacent to the beam pipe. With data from the improved backward detectors, SPACAL (H1) and BPC (ZEUS), and the shifted interaction region run in 1995, the measurements of F_2 now cover a range of Q^2 down to 0.1 GeV^2. These data allow the study of the transition region from perturbative QCD (DIS) to the photoproduction limit described by Regge phenomenology.

The low Q^2 results for F_2 from the HERA experiments are shown in Fig. 4. The ZEUS BPC data [5] collected in 1995 cover $0.11 \leq Q^2 \leq 0.65$ GeV^2 and $2 \cdot 10^{-6} \leq x \leq 6 \cdot 10^{-5}$ and are based on an integrated luminosity of 1.65 pb^{-1}. The total systematic error varies from 6% up to 11% with an overall normalization uncertainty of 2.4%. The points were extracted assuming $F_L = 0$. Using F_L obtained from the Vector Dominance Model, where $\sigma_L = (Q^2/M_V^2)\sigma_T$ and M_V is taken to be the mass of the ρ°, results in a 5-7% increase for F_2 at the highest y (lowest x). The H1 measurements [7] based on the shifted vertex running in 1995 cover $0.35 \leq Q^2 \leq 3.5$ GeV^2 and $x \geq 6 \cdot 10^{-6}$ and are based

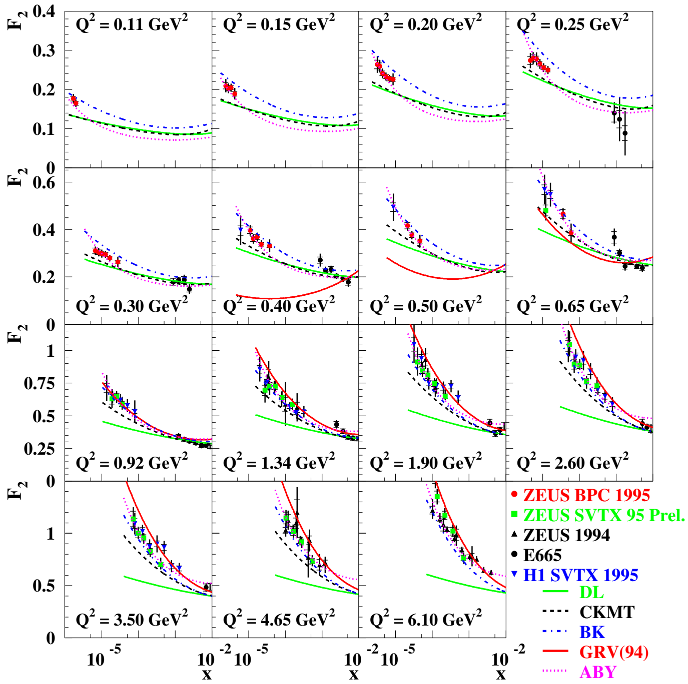

Figure 4: Recent measurements of the proton structure function $F_2(x, Q^2)$ in the low Q^2 region by H1 and ZEUS (full symbols), together with previous results from the E665 experiment. Different models are compared with the data.

on an integrated luminosity of 0.12 pb^{-1}. The total systematic and overall normalization errors are 5-10% and 3%, respectively. The preliminary ZEUS shifted vertex data [22] from the same period in 1995 cover $Q^2 > 0.65$ GeV^2. For both results obtained with shifted vertex F_L is taken from Ref. 23. In the region of overlap the results are in good agreement. The data also show a smooth continuation from the fixed target measurements towards the low x region at HERA. The rise of F_2 with decreasing x is very strong for values $Q^2 \geq 2$ GeV^2 but diminishes for smaller Q^2 values.

Several parameterizations, based on phenomenological models, are also shown in Fig. 4. One line is the prediction of Donnachie and Landshoff [4] based on a Regge inspired model, which expects the rise of F_2 to be driven by the intercept of the *Pomeron* trajectory as determined from soft hadronic interactions. The data are above this prediction already for Q^2 values greater than 0.5 GeV^2. Also shown in figure 4 are the expectations from the QCD-based GRV model [20]. This model assumes that all parton distributions have a valence like shape (i.e. vanish for $x \to 0$) at a very low $Q_0^2 = 0.34$ GeV^2 and that the leading twist QCD evolution equations can be used to evolve the parton distributions from this low Q_0^2 scale to larger values of Q^2. The GRV curve systematically undershoots the data at lower $Q^2 \leq 1$ GeV^2 while providing a fair description at higher Q^2. Other parameterizations shown in Fig. 4 use mostly ingredients from Regge theory at low Q^2 and from QCD when Q^2 is in the order of 1 GeV^2. For a recent overview see e.g. Ref. 24.

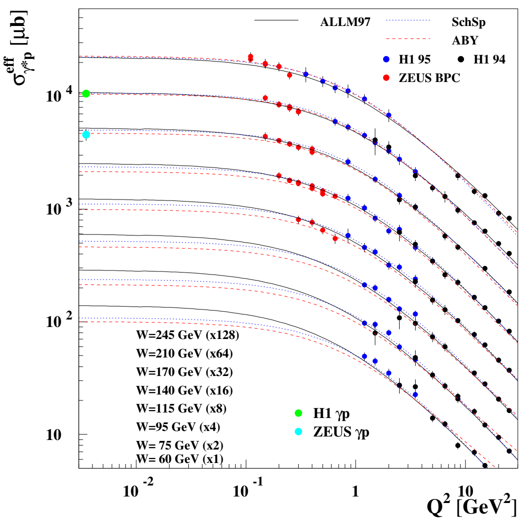

Figure 5: Measurement of the virtual photon-proton cross section $\sigma^{eff}_{\gamma^* p}$ by the HERA experiments as a function of Q^2 at various values of W, starting from the most upper curve at $W = 245$ GeV down to the bottom curve at $W = 60$ GeV. The photoproduction points as measured at HERA are also given. The curves represent different parameterizations for the transition region from DIS to the photoproduction limit ($Q^2 = 0$.)

To study the whole transition region starting from photoproduction it is convenient to present the low Q^2 data in terms of a virtual photon-proton cross section. The double differential ep cross section from Eq. (1) can be expressed via the absorption cross sections for transverse and longitudinal photons as

$$\frac{d\sigma}{dx dQ^2} = \Gamma[\sigma_T(x,Q^2) + \epsilon(y)\sigma_L(x,Q^2)] \equiv \Gamma\sigma^{eff}_{\gamma^* p}(x,Q^2), \qquad (14)$$

where the flux factor Γ is defined as $\Gamma = \alpha(2-2y+y^2)/(2\pi Q^2 x)$ and the transverse photon polarization ϵ is given by $\epsilon = 2(1-y)/(2-2y+y^2)$. The quantity $\sigma^{eff}_{\gamma^* p}$ is the effective measured virtual photon-proton cross section for ep collisions in the defined kinematic range and can be determined without any assumptions regarding F_L. At low y, where the effects of F_L are not sizeable, the effective cross section $\sigma^{eff}_{\gamma^* p}$ is identical to $\sigma^{tot}_{\gamma^* p}$, where $\sigma^{tot}_{\gamma^* p} = \frac{4\pi^2\alpha}{Q^2}F_2$.

Fig. 5 shows the experimentally determined cross section $\sigma^{eff}_{\gamma^* p}$ from H1 and ZEUS as a function of Q^2 for 8 distinct W values ($W^2 \simeq Q^2/x$) between 60 and 245 GeV. The measurements of the total photoproduction cross sections ($Q^2 \approx 0$) from HERA [25,26] are also shown. In the logarithmic representation for fixed values of W the measured cross section $\sigma^{eff}_{\gamma^* p}$ can be seen to converge to finite values as $Q^2 \to 0$. The data at low Q^2 clearly indicate a smooth transition to the photoproduction limit. The parameterizations ALLM97 [27], SchSp [28] and ABY [29] in figure 5 are recent fits to the data and can be used for a description of the transition region in the HERA kinematical range[a].

7 Summary

The H1 and ZEUS experiments at HERA have extended the previously accessible kinematic range for F_2 up to very large values of Q^2 and down to very small values of x covering the region $0.1 \leq Q^2 \leq 5000$ GeV^2 and $2 \cdot 10^{-6} \leq x \leq 0.5$. Conventional NLO QCD evolution equations have been found to provide a good description of the data down to Q^2 values as low as 1 GeV^2. The analysis of the HERA F_2 data in the framework of pQCD has led to a determination of the gluon distribution at low x. The gluon distribution is found to be steeply rising towards low x as one might expect from the strong rise of F_2 with decreasing x. Both gluon densities extracted from H1 and ZEUS data are accurate to $\sim 15\%$ at $x \sim 10^{-4}$ and are in good agreement with each other. A method used by H1 to determine the longitudinal structure function F_L has been described, yielding a broad agreement with the QCD expectation but F_L is systematically somewhat higher than expected. Although the method assumes that F_2 can be extrapolated to high y using QCD, no assumptions have been made about F_L.

[a] The parameterization ALLM97 provides an overall description of all available F_2 data in the whole x and Q^2 range studied so far.

Measurements of F_2 at very low Q^2 have also been presented. The low Q^2 values were reached by using new detector components and special runs for which HERA operated with a shifted interaction region. At very low Q^2 the rate of growth of F_2 towards low x diminishes and the data are in better agreement with models based on Regge phenomenology. In addition, the cross section measurements at low Q^2 show a smooth transition to the photoproduction regime.

Acknowledgments

I would like to thank the organizers for the wonderful conference. The work presented here represents the efforts of all the members of the H1 and ZEUS Collaborations. It is therefore a particular pleasure for me to thank all my colleagues from H1 and ZEUS. I wish to thank D. Reyna and J. Gayler for a careful reading of the manuscript.

References

1. H1 Collab., I. Abt *et al*, *Nucl. Phys.* B **407**, 515 (1993),
   ZEUS Collab., M. Derrick *et al*, *Phys. Lett.* B **316**, 412 (1993).
2. ZEUS Collab., M. Derrick *et al*, *Z. Phys.* C **69**, 607 (1996).
3. H1 Collab., S. Aid *et al*, *Nucl. Phys.* B **470**, 3 (1996).
4. A. Donnachie and P.V. Landshoff, *Z. Phys.* C **61**, 139 (1994).
5. J. Breitweg *et al*, *Phys. Lett.* B **407**, 432 (1997).
6. H1 SPACAL-Group, *Nucl. Instrum. Methods* A **374**, 149 (1996).
7. H1 Collab., C. Adloff *et al*, *Nucl. Phys.* B **497**, 3 (1997).
8. H1 Collab., Paper 262 presented at International Europhysics Conference on High Energy Physics, HEP97, Jerusalem 1997.
9. Yu.L. Dokshitzer, *Sov. Phys. JETP* **46**, 641 (1977);
   V.N. Gribov and L.N. Lipatov, *Sov. J. Nucl. Phys.* **15**, 438 and 675 (1972);
   G. Altarelli and G. Parisi, *Nucl. Phys.* B **126**, 298 (1977).
10. M.A.J. Botje, Proceedings of 5th International Workshop on Deep Inelastic Scattering and QCD, Chicago, IL, April 14-18, 1997.
11. A. Martin, R. Roberts, W.J. Stirling, *Phys. Rev.* D **50**, 6734 (1994).
12. NM Collab., P. Amaudruz *et al.*, *Phys. Lett.* B **295**, 159 (1992).
13. NM Collab., M. Arneodo *et al.*, *Nucl. Phys.* B **483**, 3 (1997).
14. BCDMS Collab., A.C. Benvenuti *et al.*, *Phys. Lett.* B **223**, 485 (1989) and *Phys. Lett.* B **237**, 592 (1989).
15. H. Georgi and H.D. Politzer, *Phys. Rev.* D **14**, 1829 (1976).

16. E. Laenen *et al.*, *Nucl. Phys.* B **392**, 162 (1993);
S. Riemersma *et al.*, *Phys. Lett.* B **347**, 143 (1995).
17. NM Collab., M. Arneodo *et al.*, *Phys. Lett.* B **309**, 222 (1993).
18. A. Martin, R. Roberts and W.J. Stirling, *Phys. Lett.* B **387**, 419 (1996).
19. H.L. Lai *et al.*, *Phys. Rev.* D **55**, 1280 (1997).
20. M. Glück, E. Reya and A. Vogt, *Z. Phys.* C **67**, 433 (1995).
21. H1 Collab., C. Adloff *et al.*, *Phys. Lett.* B **393**, 452 (1997).
22. B. Surrow, Proceedings of 5th International Workshop on Deep Inelastic Scattering and QCD, Chicago, IL, April 14-18, 1997.
23. B. Badelek, J. Kwiecinski and A. Stasto, *Z. Phys.* C **74**, 297 (1997).
24. A.M. Cooper-Sarkar, A. De Roeck and R.C.E. Devenish, DESY report 97-226, submitted to Int.J.Mod.Phys.
25. H1 Collab., S. Aid *et al.*, *Z. Phys.* C **69**, 27 (1995).
26. ZEUS Collab., M. Derrick *et al.*, *Z. Phys.* C **63**, 408 (1994).
27. H. Abramowicz, E.M. Levin A. Levy and U. Maor, *Phys. Lett.* B **269**, 465 (1991);
A. Marcus, Ph.D. thesis Tel-Aviv University, TAUP 2350-96 (1996);
H. Abramowicz and A. Levy, DESY report 97-251.
28. D. Schildknecht and H. Spiesberger, Bielefeld University BI-TP 97/25 (1997).
29. K. Adel, F. Barreiro and F.J. Yndurain, *Nucl. Phys.* B **495**, 221 (1997).